Journal of South American Earth Sciences 18 (2004) 73–88

Journal of
South American Earth Sciences

www.elsevier.com/locate/jsames

Tectonic history of the Calcatapul Formation, Chubut province, Argentina, and the "Gastre fault system"

W. von Gosen[a,*], W. Loske[b]

[a]Geological Institute, University of Erlangen-Nürnberg, Schlossgarten 5, D-91054 Erlangen, Germany
[b]Department Geosciences and Environmental Sciences, Section Geology, University of Munich, Luisenstrasse 37, D-80333 Munich, Germany

Received 1 July 2003; accepted 1 August 2004

Abstract

Field mapping, structural analysis, and U–Pb dating of rocks in the western part of the North Patagonian Massif (Argentina) yield a revised interpretation of structural evolution in the area of the 'Gastre fault system' that previously has been interpreted as an important dextral lineament. The Calcatapul Formation predominantly consists of metapyroclastic rocks and does not represent mylonites with a dextral sense of shear. The succession can be assigned broadly to the Early Paleozoic (?Silurian–Devonian). The Yancamil granite, dated here as Permian, intruded the Calcatapul Formation. Both units were affected by a first deformation under ~NE–SW compression, accompanied by a lower greenschist facies metamorphism. This Permian (–?Triassic) event took place prior to the intrusions of the Triassic Lipetrén Formation. The second deformation, with comparable compression, affected the Calcatapul Formation and Yancamil granite, as well as injected dykes of the Lipetrén Formation. Minor mylonite strips in the Lipetrén Formation intrusions display different orientations and senses of shear and do not fit with a large-scale dextral shear zone. NW–SE-striking fracture zones in this sector of the North Patagonian Massif can be interpreted also as the result of downfaulting instead of large-scale strike-slip fault lines. These observations from the Gastre area do not support the existence of the dextral Gastre fault system as a large-scale, intracontinental structural element that traverses extra-Andean Patagonia.

Keywords: Patagonia; Gastre area; Tectonics; U-Pb dating; Late Paleozoic; Triassic

1. Introduction

The North Patagonian Massif in southern Argentina (Fig. 1) is delimited by the Río Chubut in the south, the Río Negro in the north, the Atlantic coast in the east, and the foothills of the Patagonian Cordillera in the west. It consists of poorly exposed Precambrian–Early Paleozoic rocks intruded by Early to Late Paleozoic granitoids and some younger plutons. These units are covered and obscured by widely distributed Triassic to Tertiary magmatic and sedimentary rocks.

Different geotectonic interpretations have been ascribed to Patagonia. It has been interpreted as either a terrane, accreted to the southwestern margin of Gondwanan South America during the Late Paleozoic–Triassic (Ramos, 1984, 1986), or an integral part of South America since the Early Paleozoic (e.g. Dalla Salda et al., 1992a,b, 1993, 1994).

In the western part of the massif, the Central Patagonia Batholith (Rapela and Kay, 1988) is represented by scattered exposures of intrusions from the Gastre area in the southeast to the Patagonian Cordillera in the northwest (e.g. Rapela et al., 1992). The Upper Triassic–Lower Jurassic age of the intrusions has been shown by radiometric dating (e.g. Alonso, 1987; Rapela et al., 1991, 1992; Linares et al., 1997). The magmatic rocks of the batholith are distinct from the Mamil Choique Formation intrusive rocks, which are interpreted as Precambrian to Early Paleozoic and/or Late Paleozoic in age (e.g. Ravazzoli and Sesana, 1977; Proserpio, 1978b; Nullo, 1978b; Llambías et al., 1984; Rapela et al., 1992).

In the northern part of the Chubut province, the NW–SE-trending and tens of kilometers wide 'Megafalla de Gastre' (Rapela et al., 1991), 'Gastre Shear Zone System'

* Corresponding author. Tel.: +49 9131 852 2699; fax: +49 9131 852 9295.

E-mail addresses: vgosen@geol.uni-erlangen.de (W. von Gosen), wloske@iaag.geo.uni-muenchen.de (W. Loske).

0895-9811/$ - see front matter © 2004 Elsevier Ltd. All rights reserved.
doi:10.1016/j.jsames.2004.08.007

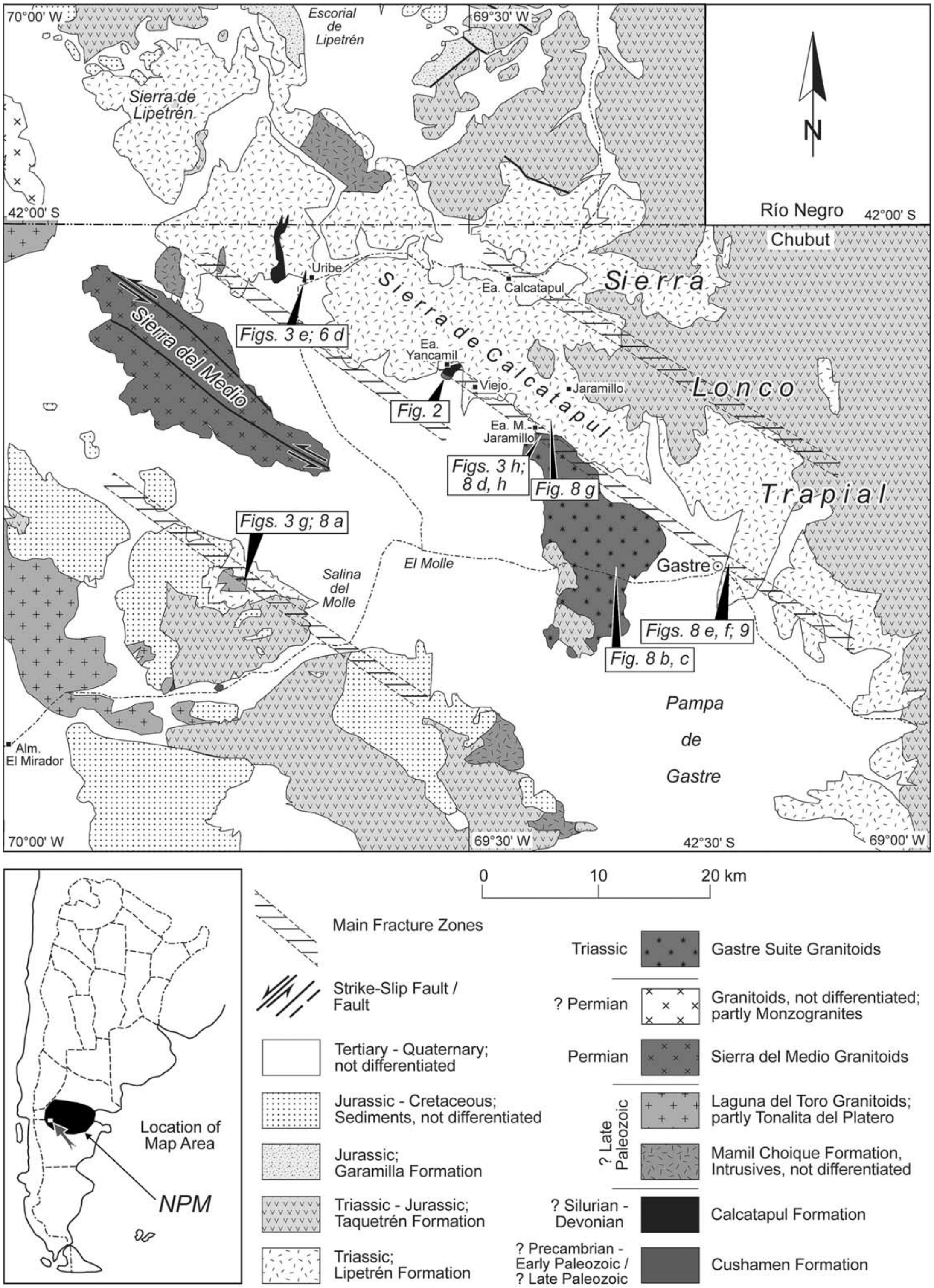

Fig. 1. Simplified geological sketch map of the Gastre-Lipetrén area in the western part of the North Patagonian Massif (Río Negro and Chubut provinces). Map is compiled after Volkheimer (1964), Nullo (1978a), Proserpio (1978a,b), Llambías et al. (1984), Rapela et al. (1992) and López de Luchi (1994), and other authors cited in the text. Inset map shows the location of the map area in the North Patagonian Massif (NPM). Locations of various figures also are indicated.

(Rapela et al., 1992), or 'Gastre Fault System' (Rapela and Pankhurst, 1992; Rapela, 1997) has been hypothesized, partly based on the 'Gastre System' of fractures described by Coira et al. (1975). The existence of the fault system in the Sierras de Calcatapul and Lonco Trapial, near the village of Gastre (Fig. 1), has been based on fracture zones and mylonites with a dextral sense of shear (e.g. Rapela et al., 1991, 1992; Rapela, 1997). However, Franzese and Martino (1998) describe an oblique reverse displacement with a sinistral component from a mylonite in this area.

Rapela et al. (1992) and Rapela and Pankhurst (1992) propose that movements along the fault zone were related to intracontinental dextral shearing during the Late Triassic–Early Jurassic, followed by a large-scale transfer (∼400–500 km) of the southern, intra-Patagonian block during Early to Mid-Jurassic times. They interpret the emplacement of the intrusions in the Gastre area as synchronous with the developing fault system and postulate that NW–SE-striking equivalents of the fault system continue northwest into the Patagonian Cordillera. Beyond a cover of Upper Jurassic and younger sedimentary sequences, the fault system was thought to appear again at the Atlantic coast (∼45°S), associated with volcanic rocks of the Marifíl Group.

In the working hypothesis of Rapela et al. (1992), Rapela and Pankhurst (1992), and Rapela (1997), the Gastre fault system was a tool for plate tectonic interpretations of the South American–South African separation. It has been interpreted as a precursor and onshore continuation of the Falklands–Agulhas Fracture Zone. Later plate tectonic reconstructions that focus on the fragmentation of southern Gondwana include the Gastre fault system as an important structural element in southern South America (e.g. Marshall, 1994; Richards et al., 1996; Watkeys and Sokoutis, 1998).

In this article, we report new evidence from the area between the village of Gastre and the northern part of the Sierra de Calcatapul (Fig. 1). The results shed doubt on the existence of the Gastre fault system as it has been proposed in previous interpretations, particularly in terms of the dextral sense of displacement, intracontinental dimensions, and plate tectonic importance. The evidence leads to a different structural interpretation of that area in the western part of the North Patagonian Massif.

2. Lithological units

In the Gastre area, the Cushamen Formation is exposed in two small areas (Fig. 1). Its metapsammitic to metapelitic succession has been interpreted as Precambrian and/or Early Paleozoic in age (e.g. Volkheimer, 1964, 1973; Ravazzoli and Sesana, 1977; Proserpio, 1978b; Volkheimer and Lage, 1981; Llambías et al., 1984; Dalla Salda et al., 1990; Ostera et al., 2001). Duhart et al. (2002), however, provide evidence of a Late Paleozoic age for at least parts of the Cushamen Formation.

Northwest of the village of Gastre, at the western margin of the Sierra de Calcatapul and to the northwest (Fig. 1), a distinct lithological unit, mentioned by Volkheimer (1965), was mapped, described, and named as Calcatapul Formation by Proserpio (1978a,b). Its simply deformed, low-grade metamorphic rocks (Proserpio, 1978b; Nullo, 1978b) are exposed in two occurrences indicated on the overview maps of Proserpio (1978a) and Nullo (1978a) and an additional small occurrence just west of Puesto Uribe (Fig. 1).

According to Proserpio (1978b) and Nullo (1978b), the Calcatapul Formation mostly consists of acid to intermediate metapyroclastic and volcanic rocks. In the area of

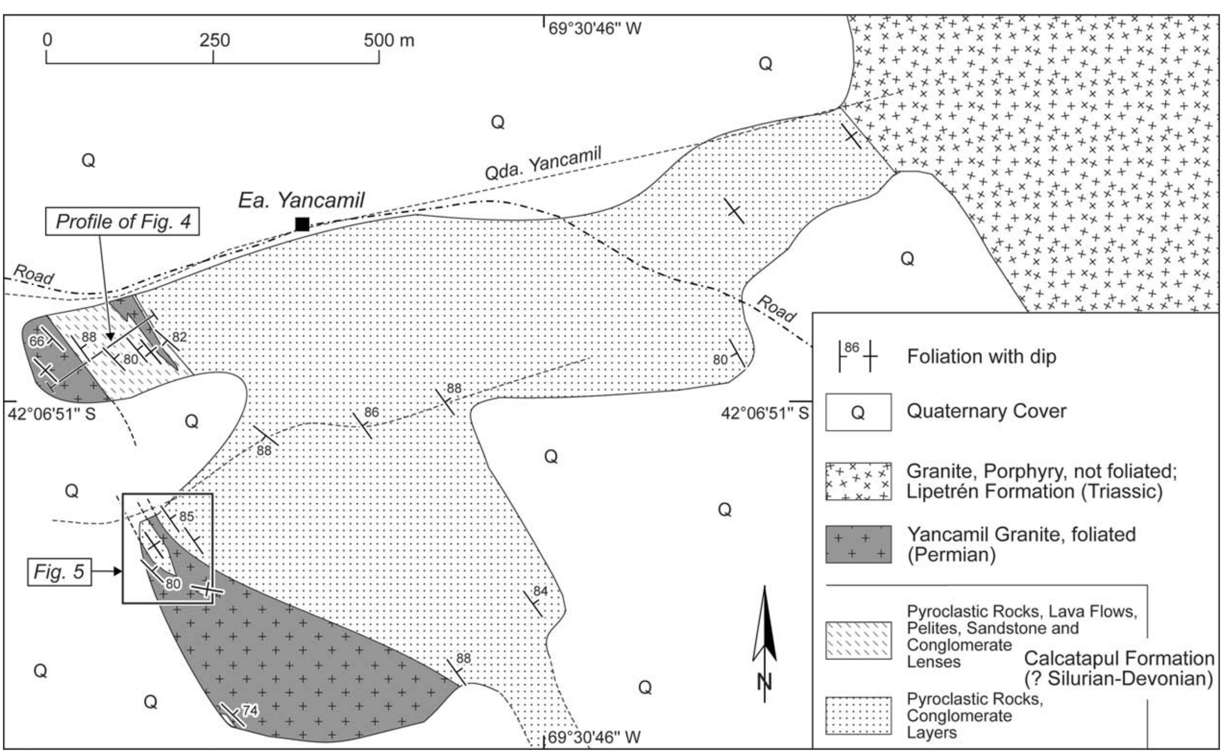

Fig. 2. Simplified geological map of the Calcatapul Formation and adjacent intrusions in the Yancamil area at the western slope of the Sierra de Calcatapul. Map is based on field mapping. For location, see Fig. 1. The line of the profile in Fig. 4 and location of the sketch map in Fig. 5 are indicated.

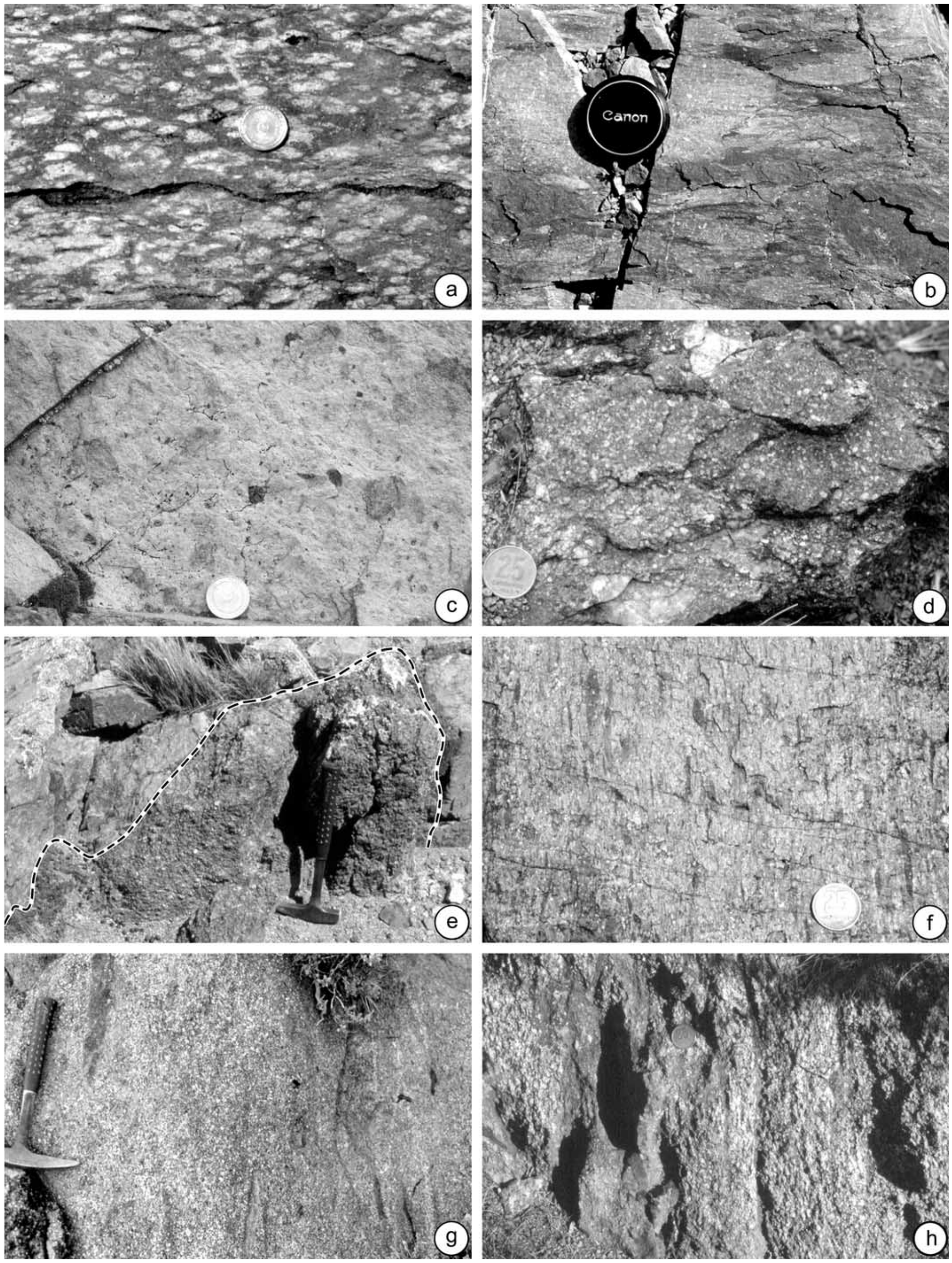

Fig. 3. Details from the Calcatapul Formation in the Yancamil area (a–d and f, east of Quebrada Yancamil) and various granitoids of the Gastre area (e, g, h). (a) Metapyroclastic rock with feldspar-rich lapilli elongated in the S_1 foliation. Plan view, upper side of photograph = NE. (b) Metaconglomerate in the metapyroclastic succession containing pebbles of rhyolitic to dacitic (light) and pyroclastic (dark) rocks. Plan view, upper side of photograph = ~SW. (c) Fine-grained pyroclastic rock with angular rock fragments. View to SW. (d) Metaconglomerate with rounded to subangular pebbles of polycrystalline quartz. View to ~SE. (e) Block of diffusely foliated granite (center) in light porphyries of the Lipetrén Formation. Contact is marked by a dashed line; hammer is oriented parallel to the trace of the weak foliation (view to ~SW, west of Puesto Uribe; for location, see Fig. 1). (f) View to SE on trace of S_1 foliation plane in metapyroclastic rock with elongated lapilli and various clast types. (g) View to SW on trace of the weak and diffuse foliation in Laguna del Toro granodiorite to tonalite. Note lens-shaped mafic enclaves in the intrusion (west of Salina del Molle; for location, see Fig. 1). (h) View to ~SE on trace of subvertical and weak foliation in Gastre suite granite SE of Estancia Jaramillo (coin in the upper central part for scale; for location, see Fig. 1).

the Quebrada Yancamil (NW of Gastre; Fig. 2), these dominant rock types contain layers with accumulated lapilli (lens-shaped, feldspar-rich aggregates on a mm to cm scale; Fig. 3a), some rhyolite layers, and conglomerates. The latter contain pebbles of mudstones, pyroclastic rocks, and rhyolites of mm to dm sizes (Fig. 3b). The pyroclastic rocks occupy the entire northeastern part of the Calcatapul Formation near Estancia Yancamil (Fig. 2). Fine-grained

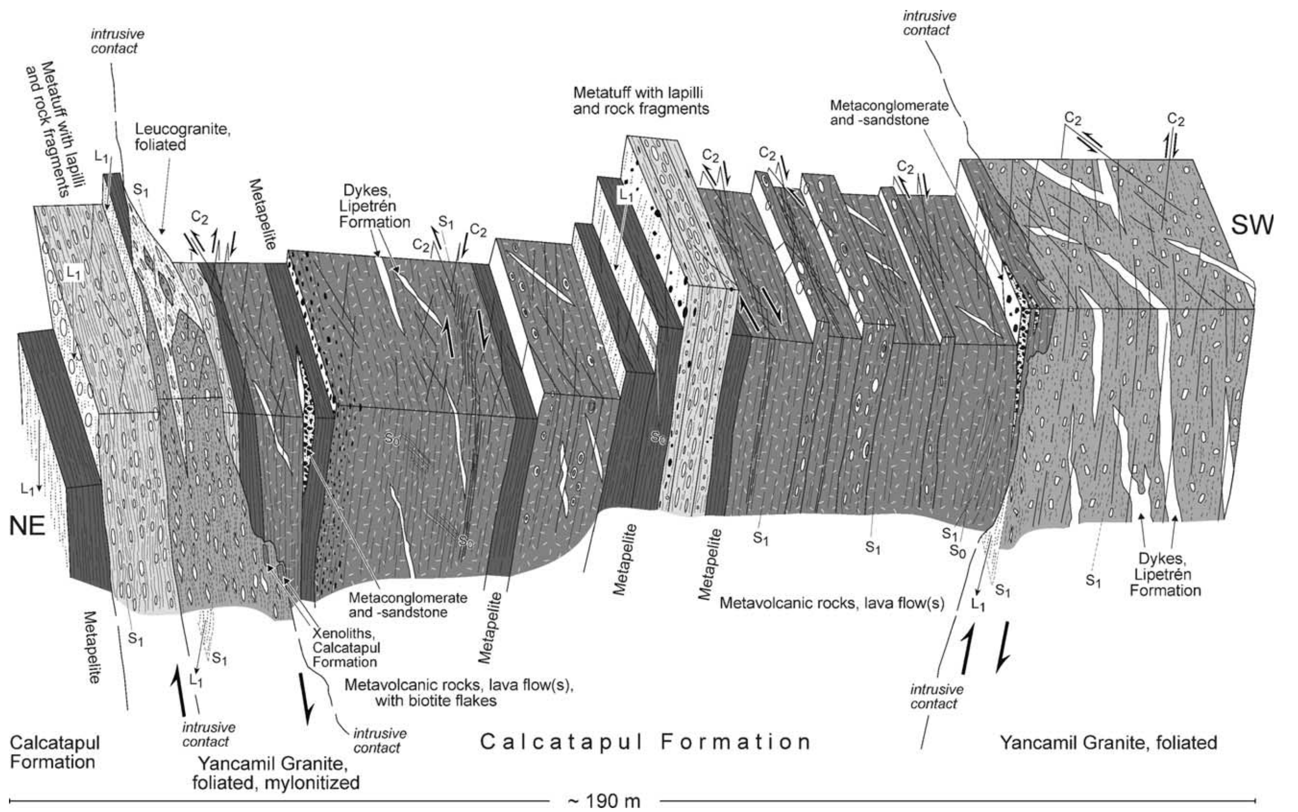

Fig. 4. Simplified schematic block profile across the southwestern part of the Calcatapul Formation in the Yancamil area (for location, see Fig. 2). Note S_1 foliation cutting across the intrusive contacts of the Yancamil granite in the southwest and northeastern part of the section. The L_1 lineation is subvertical. A conjugate set of dextral and sinistral C_2 planes also cross-cuts the dykes of the Lipetrén Formation and is locally condensed with a dominant dextral sense of shear.

varieties contain angular rock fragments of mm to cm sizes (see also Proserpio, 1978b; present Fig. 3c). In the southwestern part of the Formation, thick layers of metavolcanic rocks represent lava flows (Fig. 4) separated from one another by several m thick layers of dark phyllitic mud-/siltstone. In addition, dm-thick lenses of sandstones with quartz-conglomerates occur (Figs. 3d and 4).

According to the subvertical orientation of the main foliation, mostly parallel to the compositional layering (relic of bedding), the Calcatapul Formation is at least 1 km thick in the Yancamil exposure, without taking into account possible repetitions by folding. An along-strike continuation to the southeast is possible but not substantiated. There are no fossils reported from the unit, and such relics could not be found during our fieldwork. A (?) Middle Paleozoic (?Silurian, ?Devonian) age of the Formation was assumed by Proserpio (1978a,b).

In the area of Yancamil, the deformed Calcatapul Formation also has been interpreted as mylonites. Together with additional occurrences, these were used as an essential argument for the existence of the dextral Gastre fault system (e.g. Rapela et al., 1991, 1992). Along its southwestern margin, the Formation is intruded by a coarse-grained granite (Figs. 2 and 4), which shall be named Yancamil granite. Slices of pyroclastic rocks were enclosed by the granite just south of the irregular, ~NW–SE-striking intrusive contact and farther southeast (Figs. 2, 5 and 6a). A later leucogranite facies intruded a dyke of the granite and the country rocks. Both types of intrusion are foliated together with the Calcatapul Formation rocks.

In the area of Gastre, a suite of various granodiorites and granites has been named the "Gastre Suite" (or "superunit") and dated as 220 ± 3 Ma (Rb–Sr, whole-rock) by Rapela et al. (1992). In several outcrops from Gastre to the northwest of Sierra de Calcatapul (west of Puesto Uribe), m- to 10 m-wide blocks of weakly foliated granites are enclosed by younger intrusive rocks of the Lipetrén Formation (Fig. 3e). The latter is widely distributed from Gastre to the northwestern parts of Sierra de Calcatapul and farther northwest (Fig. 1). It has been interpreted as Permian or Permo-Triassic in age (e.g. Proserpio, 1978b; Nullo, 1978b, 1979; Volkheimer and Lage, 1981; Cucchi, 1993). The Formation consists of various unfoliated granites, rhyolites, porphyries, and aplites. The rocks have been collectively assigned to the "Lipetrén Suite" (or "superunit") and dated as 208 ± 1 Ma (Rb–Sr, whole-rock) by Rapela et al. (1992). They intrude the Calcatapul Formation (Fig. 2) and lead to contact metamorphism of the northern occurrence (Nullo, 1978b). Injected dykes of its porphyries, mentioned by Proserpio (1978b), cut across the steeply inclined succession and Yancamil granite intrusion (Fig. 4). The dykes mostly strike between W–E and NW–SE (Fig. 6b).

The Triassic ages of the igneous rocks of both suites (based on Gradstein and Ogg's, 1996 time scale), however,

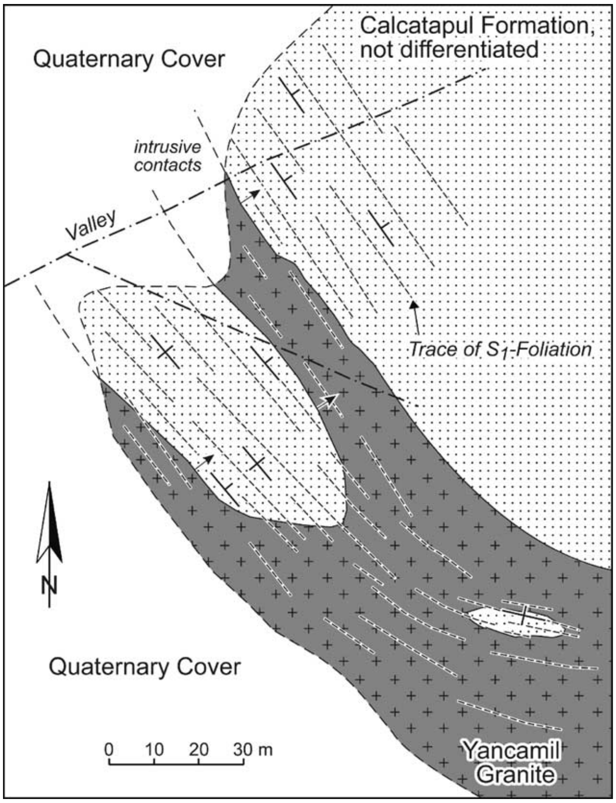

Fig. 5. Simplified sketch map of the irregular contact between the Calcatapul Formation and intruded Yancamil granite east of Quebrada Yancamil, based on field mapping (for location, see Fig. 2). Small arrows depict the steep dip of the contact.

should be considered in light of a new dating of the Taquetrén Formation performed by Franzese et al. (2002), which yields a Lower Triassic age (242.9 ± 2.5 Ma, U–Pb, zircon, SHRIMP). Its volcanic rocks and sediments, which overlie the Lipetrén Formation rocks (Fig. 1), previously were assigned to the Upper Jurassic (Nullo and Proserpio, 1975; Proserpio, 1978b). As Franzese et al. (2002) point out however, the Taquetrén Formation includes products of at least two different magmatic events (Triassic, Jurassic), and a redefinition of its age and areal extent is necessary. The Taquetrén Formation is overlain by Garamilla Formation volcanic rocks (Nullo, 1978b), which yield a Jurassic age (188.1 ± 1.5 Ma, U–Pb, zircon, SHRIMP, Franzese et al., 2002). In view of the new results and on the basis of the geological situation, we assume that parts of the Lipetrén Formation have a greater age.

The Mamil Choique Formation intrusions occur north and southeast of Sierra del Medio (Fig. 1). Former age estimates for the granitoids of this Formation span the Precambrian-Late Paleozoic interval (e.g. Ravazzoli and Sesana, 1977; Nullo, 1978b, 1979; Proserpio, 1978b; Dalla Salda et al., 1994). A radiometric date from a granodiorite gneiss of the Sierra del Medio Granitoids yields 267 ± 27 Ma (Rb–Sr, whole-rock, isochron, Rapela et al., 1992). Similar Permian ages have been reported from intrusions at Mamil Choique (NW of Gastre; e.g. Linares et al., 1997; López de Luchi et al., 2000) and the areas of Comallo and Paso Flores (Varela et al., 1999), which are located more than 150 km northwest of Gastre. These ages suggest that the Mamil Choique Formation intrusions, at least in parts, are Late Paleozoic (Permian) in age, as is also supported by the dating of the granites at Río Collón Curá (Linares et al., 1988).

In the Gastre area, the Laguna del Toro Granitoids (Rapela et al., 1992) correspond to the Tonalita del Platero (Volkheimer, 1964) or El Platero Formation (Volkheimer and Lage, 1981) exposed in the western areas. According to an isotopic date of a tonalite approximately 10 km NNW of Almacén El Mirador (280 ± 10 Ma, Proserpio, 1978b) and a poorly defined Rb–Sr whole-rock date of a biotite granodiorite gneiss west of Gastre (346 ± 35 Ma, Rapela et al., 1992), it is possible that at least parts of the El Platero Formation, Laguna del Toro granitoids, and Sierra del Medio granitoids belong to the same Late Paleozoic plutonism. A preliminary Rb/Sr isochron from the El Platero tonalite, however, yields 211 ± 10 Ma (Linares et al., 1997) and suggests that parts of this group of intrusions are younger.

3. Structures in the Calcatapul Formation and intrusives

3.1. D_1 deformation

Within the Calcatapul Formation at Estancia Yancamil, a penetrative but heterogeneously developed S_1 foliation affects all rock types, along with various clasts and lapilli (Figs. 3f and 4). In the entire area, S_1 planes strike NW–SE and steeply dip to the SW or NE or are vertical (see also Proserpio, 1978b). On S_1 planes, a pronounced L_1 lineation is indicated by aligned sericite, pressure shadows at clasts, lens-shaped elongated lapilli, and stretched, disrupted, and extended clasts. It steeply plunges ~SW or ~NE or is vertical (Fig. 6c). We found no evidence for a gently plunging or subhorizontal orientation of L_1. West of Puesto Uribe, the L_1 lineation plunges E to ENE (Fig. 6d).

In a few places in the Yancamil section, we detected relics of S_0/S_1 cross-cutting relationships (Fig. 4). The intersection lineation strikes ~NW–SE (Fig. 6e). In most places, S_1 planes are parallel to bedding planes. Neither F_1 folds nor way-up indicators were found.

At the southwestern margin of the Calcatapul Formation, the S_1 foliation cuts across the intrusive contact of the Yancamil granite (Fig. 4) and through a slice of the pyroclastic rocks enclosed by the granite (Fig. 5). To the southwest, however, the foliation in the granite is weakly and heterogeneously developed, as in the metavolcanic rocks (lava flows) of the Calcatapul Formation northeast of the contact. One dyke of the granite in the Calcatapul Formation rocks (Fig. 4), along with a leucogranite in its central part, is penetratively foliated and partly mylonitized. As in the main granite body, the steeply plunging L_1 lineation is recorded by

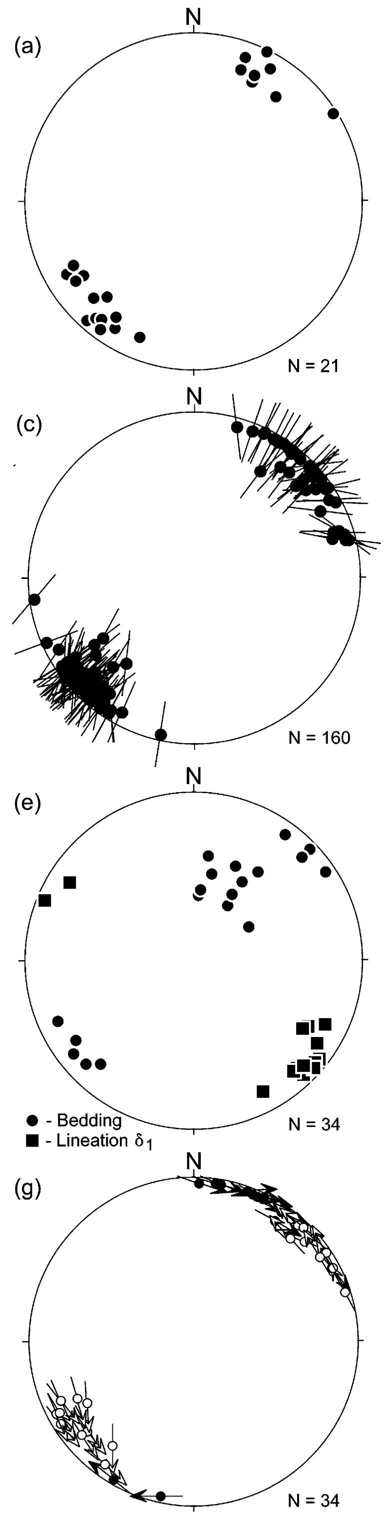

Fig. 6. Lower hemisphere, equal area stereoplots of structural elements in the Calcatapul Formation and intrusions of the Yancamil area except (d), which is from the exposure west of Puesto Uribe (for location, see Fig. 1). (a) Contact planes between Yancamil granite and Calcatapul Formation. (b) Orientation of dykes of the Lipetrén Formation in the foliated Calcatapul Formation and Yancamil granite. (c and d) L_1 lineation on S_1 planes in the Calcatapul Formation (Hoeppener plots). (e) Bedding planes and intersection lineation in the Calcatapul Formation. (f) L_1 lineation on S_1 planes with a southwest-directed relative sense of shear in the foliated Yancamil granite (Hoeppener plot). (g and h) Hoeppener plots of slickensides on dextral (white) and sinistral (black) C_2 shear planes in the Calcatapul Formation (g) and Yancamil granite (h). In all Hoeppener plots (Hoeppener, 1955), the lineation is projected on the respective pole of the plane, and arrows indicate the relative sense of shear of the hangingwalls.

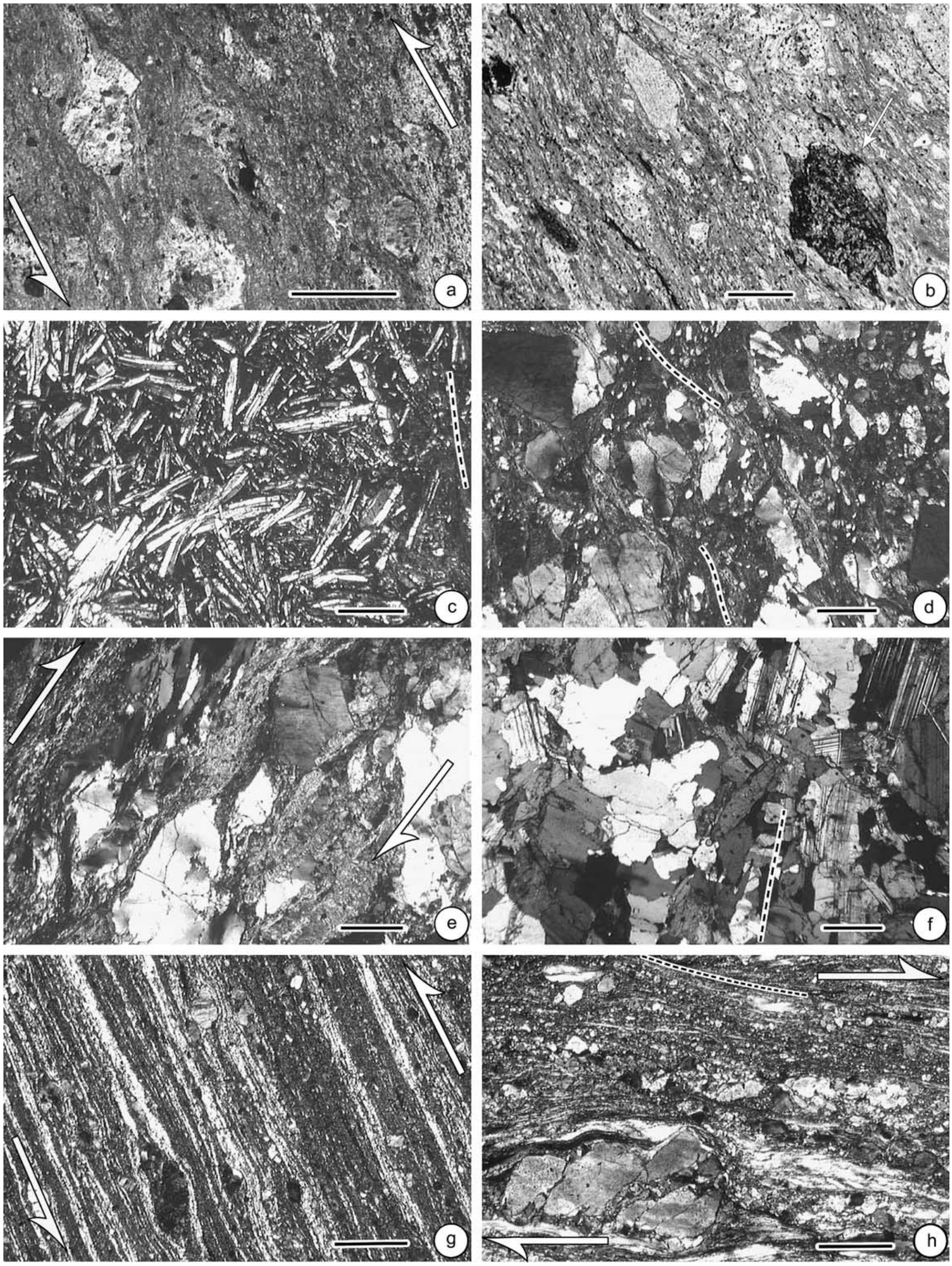

Fig. 7. Photomicrographs from thin sections; 1 mm scale bars; crossed polarizers except (a) and (b) with plane polarized light. (a) Metatuff from the Calcatapul Formation east of Quebrada Yancamil (NW of Gastre). Clasts of single feldspar grains and polycrystalline aggregates (lapilli) depict asymmetric σ-shapes of pressure shadows in the penetrative S_1 foliation. Relative sense of shear is reverse (ENE side up), shown by half arrows. (b) Metatuffitic rock from the Calcatapul Formation in Yancamil (east of Quebrada Yancamil). Various clasts of feldspar, feldspar aggregates, and dark volcanic rocks (arrow) are affected by the penetrative S_1 foliation. (c) Metavolcanic rock (lava flow) from the southwestern part of the Calcatapul Formation (east of Quebrada Yancamil). Plagioclase ledges display relics of intersertal textures in a dense matrix. They are partly bent, kinked, or broken due to the D_1 deformation. Orientation of trace of S_1 planes at the right side is depicted by thin dashed line. (d) Metaconglomerate from the southwestern part of the Calcatapul Formation (east of Quebrada Yancamil). Deformed pebbles of feldspar, single, and polycrystalline quartz are affected by the sericite-rich S_1 foliation (indicated by dashed lines). (e) Mylonitized Yancamil granite southeast of Quebrada Yancamil. σ-shapes of ductilely deformed quartz lenses and pressure shadows at feldspar clasts record a reverse sense of shear (NE side up), shown by half arrows. (f) Laguna del Toro tonalite to granodiorite west of Salina del Molle (W of Gastre). The trace of

elongated quartz and aligned muscovite/sericite and has the same orientation as that of the country rocks.

The observations suggest that both the Calcatapul Formation and the Yancamil granite intrusion were affected by ~NE–SW compression. The entire succession has been elongated parallel to the steeply plunging to subvertical L_1 lineation. Because of the heterogeneous foliation development, the section at Yancamil does not represent a mylonite zone. Only parts of the Yancamil granite and some metapyroclastic layers were affected by mylonitization.

3.2. Microfabrics and metamorphism

3.2.1. Calcatapul Formation

In the metapyroclastic rocks, the penetrative S_1 foliation is recorded by aligned sericite. The matrix consists of finest-grained feldspar and dynamically recrystallized quartz. Angular porphyroclasts of K-feldspar, single quartz grains, and feldspar aggregates are affected by stretching. They are partly disrupted and/or displaced within the foliation. Pressure shadows are filled with quartz, sericite, and ±chlorite. Only some layers can be described as mylonites, whereas most parts display a penetrative S_1 foliation.

Single quartz grains in the matrix do not record corrosion phenomena. Small lenses are filled with coarser quartz and/or feldspar (Fig. 7a), partly converted into epidote and clinozoisite, and interpreted as lapilli. This is also assumed for some (polycrystalline) clasts that consist of plagioclase and K-feldspar within a finest-grained matrix of quartz. Clasts with randomly oriented plagioclase ledges in a finest-grained matrix (see also Proserpio, 1978b) filled with dense opaque dust (Fig. 7b) are directly comparable to lava flows. Others consist of either sericite and a fine-grained matrix of quartz or coarser-grained quartz and feldspar (compare Proserpio, 1978b). Sericite flakes often are impregnated by opaque dust and also point to a clastic input within dacitic to rhyodacitic volcanic rocks.

In the southwestern part of the Yancamil section, the metavolcanic rocks display a dense fabric of plagioclase ledges that record (relics of) intersertal and partly fluidal textures (Fig. 7c) and therefore are interpreted as lava flows. The finest-grained matrix consists of quartz, chlorite, and microbiotite and is densely filled with opaque grains and dust. Lenses and thin layers in the rocks are filled with quartz, plagioclase, and microbiotite ± sericite. They could represent amygdaloidal textures, whereas other lenses, filled with coarse-grained quartz and feldspar, are interpreted as rock fragments. Lens-shaped biotite aggregates with diffuse boundaries could be derived from mafic minerals, though these are not preserved. Also on the basis of the field observations, we assume that these lava flows represent diabase (spilites) or trachytic volcanics. We found no evidence to postulate dykes.

The volcanic rocks are heterogeneously affected by the S_1 foliation. The magmatic texture is cross-cut by single S_1 planes (Fig. 7c), and plagioclase is successively rotated into these planes. Such areas can change into those in which a clear foliation is developed. There, plagioclase is bent, kinked, and broken, and spaces between the dismembered fragments are filled with quartz and/or biotite. The latter is grown parallel to the S_1 planes.

Within the thin lenses of metaconglomerates, a penetrative S_1 foliation is recorded by aligned sericite, chlorite, and ±microbiotite and is not mylonitic (Fig. 7d). Quartz and feldspar exhibit ductile and brittle deformation, respectively. Dynamically generated quartz recrystallization grains occur in the matrix. Single clastic biotite is replaced by recrystallization grains. The microstructures in the metapelitic layers are directly comparable. There, the cross-cutting relationship between bedding (S_0) and S_1 foliation follows that found in the field.

The pebble content of the metaconglomerates can be assigned to several groups. Coarse K-feldspar clasts, partly with micrographic intergrowths, may be related to eroded intrusions. Single quartz grains with corrosion phenomena probably were derived from acid volcanics. As in the metapyroclastic rocks, single polycrystalline quartz pebbles internally consist of coarsely recrystallized quartz grains deformed by the S_1 foliation. These clasts originated from a metamorphic complex. In the metapelitic layers and some metapyroclastic rocks, single flakes of mudstones, impregnated by opaque dust, were derived from a sedimentary complex.

The clasts' content supports the field observations that the metapyroclastic rocks are tuffs to tuffites (see also Volkheimer, 1965; Proserpio, 1978b; Nullo, 1978b) with variable contents of volcanic and clastic debris. In this part of the Formation, pebbles also are accumulated within conglomerate layers. These clasts are affected by the penetrative S_1 foliation and do not record an older foliation fabric. Except for those from a metamorphic complex, they probably were derived from the local succession.

3.2.2. Yancamil granite

In the interior, southwestern parts of the granite, sericite grew parallel to weakly developed S_1 planes. Magmatic quartz is elongated with sericite ± chlorite

a diffuse foliation (marked by dashed line) is roughly indicated by long axes orientations of plagioclase and partly an elongation of quartz. (g) Gastre mylonite from thin strip east of Gastre village. Asymmetric σ-shapes of pressure shadows at feldspar clasts depict (oblique) reverse sense of shear (half arrows) in the west-dipping S_{my} foliation. Section is perpendicular to S_{my} foliation and parallel to L_{my} lineation (right margin = NW). (h) Gastre mylonite from a thin strip in the Lipetrén Formation northeast of Estancia Jaramillo (NW of Gastre). Displaced fragments of a broken feldspar clast and shear band (dashed line) depict a dextral sense of shear (half arrows) in the WSW-dipping S_{my} foliation. Section is perpendicular to S_{my} and parallel to gently plunging L_{my} lineation (left margin = SSE).

beards in pressure shadows and records incipient dynamic recrystallization. In the marginal parts of the granite, quartz is ductilely elongated within the penetrative, partly mylonitic S_1 foliation and contains finest-grained, dynamically generated recrystallization grains. K-feldspar and plagioclase exhibit brittle deformation, and incipient fine-grained recrystallization is detected only in high-strain areas. Magmatic biotite and muscovite are affected by shearing and replaced by microbiotite and sericite, respectively.

In the granite/leucogranite dyke, the partly mylonitic foliation is recorded by extremely elongated quartz that records subgrain formation and dynamic recrystallization. Feldspar exhibits brittle deformation.

The microstructures suggest that the Yancamil granite was affected by a heterogeneous, solid-state deformation after cooling. The deformation took place under lower greenschist facies metamorphic conditions that also appear in the Calcatapul Formation rocks, as shown by the growth of sericite + chlorite ± biotite, the dynamic recrystallization of quartz, and the mostly brittle deformation of feldspar in both units. According to Nullo (1978b), deformation and metamorphism took place prior to the intrusion of the Lipetrén Formation magmatic rocks. Other than in parts of the Yancamil granite and some layers of the pyroclastic rocks, where shearing is intensified and mylonites occur, the heterogeneously foliated rock succession generally cannot be interpreted as mylonites.

3.3. Sense of shear

At and near the contact with the Calcatapul Formation, σ-shapes of feldspar clasts within the S_1 foliation of the Yancamil granite indicate a top-to-southwest sense of shear parallel to the steeply plunging L_1 lineation (Figs. 4 and 6f). Comparable feldspar σ-clasts within the granite dyke support this uplift of the northeastern block parallel to the pronounced L_1 lineation (Fig. 4). On the microscale, this relative sense of shear is supported by σ-shapes of polycrystalline quartz lenses (Fig. 7e), pressure shadows at feldspar porphyroclasts, displaced feldspar clasts, S/C fabrics, and micro shear bands.

Microscale shear sense indicators in the metapyroclastic rocks of the Calcatapul Formation are asymmetric σ-shapes of pressure shadows (Fig. 7a), displaced porphyroclasts, and some S/C fabrics. They are comparable to σ-shapes of pressure shadows at single plagioclase grains and quartz-feldspar lenses and displaced plagioclase grains in the metavolcanic rocks. In the metaconglomerates, some asymmetric σ-shapes of pressure shadows occur.

All macro- and microscale shear sense indicators in the different lithological units prove a general uplift of the northeastern blocks parallel to the steeply plunging L_1 lineation. No evidence for a dextral sense of shear was found.

3.4. D_2 deformation

The D_1 structures in the Calcatapul Formation and Yancamil granite are cross-cut by a conjugate set of steeply inclined to subvertical, dextral and sinistral, C_2 shear planes (Figs. 4 and 6g and h). Their relative sense of shear is depicted by subhorizontal slickensides. Both planes are spaced on the dm scale. In some m-wide parts of the outcrops, however, they are condensed to the cm scale. There, both plane sets are rotated toward the finite orientation of the S_1 foliation planes, and the ~NW–SE-striking dextral planes partly dominate (Fig. 4).

The conjugate set of C_2 planes also cuts across cm- to dm-thick rhyolitic to granitic dykes of the Lipetrén Formation, which intruded the Yancamil granite and Calcatapul Formation rocks after the ductile D_1 deformation (Fig. 4). These planes are the first deformational structures in the dykes. At the northeastern margin of the Calcatapul Formation, the conjugate set of C_2 planes also cuts across the Lipetrén Formation magmatic rocks, which intruded the vertical Calcatapul Formation succession. On the basis of the orientation of the set of dextral and sinistral C_2 planes (Fig. 6g and h), we can estimate a NE–SW compression with a subhorizontal orientation of σ_1.

4. Laguna del Toro and Gastre suite granitoids

Southwest of Sierra de Calcatapul, west of Salina del Molle, a tonalite to granodiorite of the Laguna del Toro Granitoids (Rapela et al., 1992) is exposed in an area mostly occupied by rocks of the Lipetrén Formation (Fig. 1). The rocks record a weak, diffuse foliation in which lens-shaped mafic enclaves occur (Fig. 3g). The steeply inclined to vertical foliation strikes N–S to NE–SW. Poorly developed feldspar σ-clasts display an oblique sinistral sense of shear (Fig. 8a) parallel to the weak lineation recorded by aligned feldspar, amphibole, and biotite.

On the microscale, the poorly defined foliation does not record evidence of a clear solid-state deformation (Fig. 7f). Plagioclase, biotite, and, partly, amphibole depict a weak alignment of the long axes. Coarse-grained magmatic quartz is elongated only in some parts and can contain single, coarse recrystallization grains. The partial conversion of biotite into chlorite, undulatory extinction of quartz, and bending of single plagioclase can be assigned to the effects of a younger slight deformation. The structures in the outcrop suggest that the intrusion was deformed during emplacement and/or cooling.

A comparable mechanism is reasonable for the studied Gastre Suite granites. West of Gastre, a hornblende-biotite granite, described by Rapela et al. (1992), depicts a diffuse and steeply NE-dipping foliation with a weak lineation (Fig. 8b). Clear shear sense indicators could not be found. A cross-cutting conjugate set of subvertical, ~N–S- and

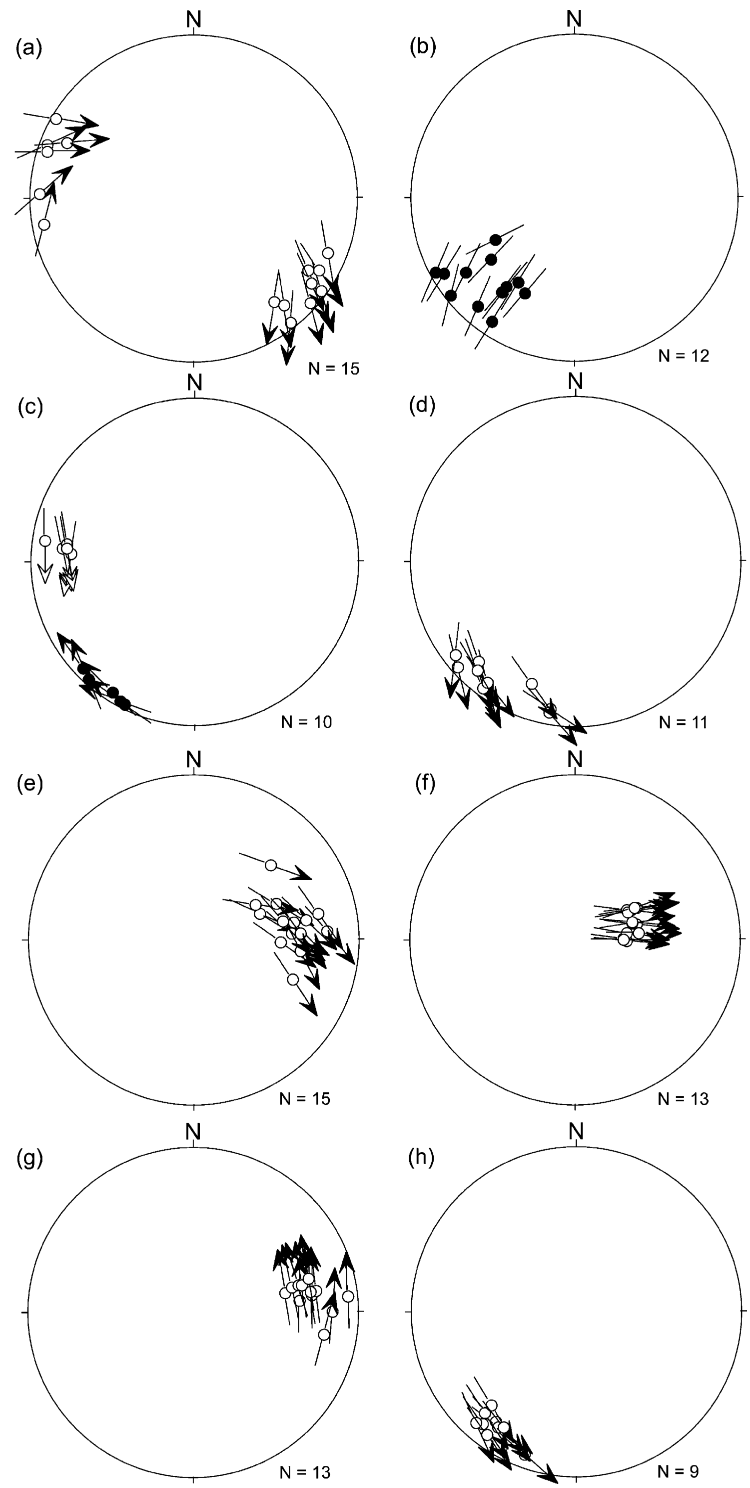

Fig. 8. Lower hemisphere, equal area Hoeppener plots of S-planes and related lineations in granitoids (a–d) and mylonite strips (e–h) of the Gastre area and surroundings (for locations, see Fig. 1). (a) Laguna del Toro granodiorite-tonalite west of Salina del Molle. (b and c) Gastre suite granite west of Gastre. (d) Gastre suite granite southeast of Estancia M. Jaramillo. Mylonite foliation and lineation in outcrops east of Gastre (e, f) and northeast (g) and southeast (h) of Estancia M. Jaramillo. In the Hoeppener plots (Hoeppener, 1955) the lineation is projected on the respective pole of the foliation plane; arrows indicate the relative sense of shear of the hangingwalls.

NW–SE-striking dextral and sinistral shear planes, respectively, broadly indicate ENE–WSW compression (Fig. 8c). This deformation affected the intrusion after the formation of the diffuse foliation fabric. The conjugate set of shear planes can be broadly compared to the C_2 plane set in the Calcatapul Formation and Yancamil granite. A comparable granite NW of Gastre, however, displays a NW–SE- to WNW–ESE-striking, diffusely developed foliation (Fig. 3h). Single feldspar σ-clasts indicate an oblique dextral sense of shear (Fig. 8d).

The few granitoids studied do not demonstrate a consistent overall trend of structures or sense of shear. Their diffuse foliations suggest that they were affected by compression during emplacement and/or cooling (magmatic foliation of Rapela et al., 1991 and Rapela and Pankhurst, 1992). However, we could find no clear indication of a direct relation with a developing Gastre fault system. Some parts could represent equivalents of the weakly foliated granites enclosed by the unfoliated intrusive rocks of the Lipetrén Formation.

5. Gastre mylonites

East of the village of Gastre, an approximately 30 m thick mylonite strip is exposed within porphyries and fine-grained granites of the Lipetrén Formation (Fig. 1), which contain blocks of a weakly foliated granite. The dark mylonite zone strikes ∼N–S and dips to the ∼W (Fig. 9). Feldspar σ- and δ-clasts, and single S/C fabrics in the mylonite foliation (S_{my}) indicate an uplift of the western block parallel to the mylonite lineation (L_{my}) but with a sinistral component (Fig. 8e). This mylonite zone was the thickest strip found in the entire area. A nearby ∼3 m thick mylonite strip in the Lipetrén Formation also dips to the west and records a top-to-east sense of shear (Fig. 8f). It should be noted that Nullo (1978b) also mentions mylonite strips in the Lipetrén Formation that record a dip between 85 and 90° to the east.

Northwest of this location, NE and SE of Estancia Jaramillo, we found two additional ∼20 cm thick mylonite strips (Fig. 1). The first one, in the Lipetrén Formation, strikes N–S and dips steeply ∼W. It records a dextral sense of shear (Fig. 8g) and laterally thins out in the porphyric rocks. The second, a ∼NW–SE striking mylonite strip in the Gastre suite granite, indicates a dextral sense of shear (Fig. 8h) that follows that of the weak older foliation at the same locality (cf. Fig. 8d).

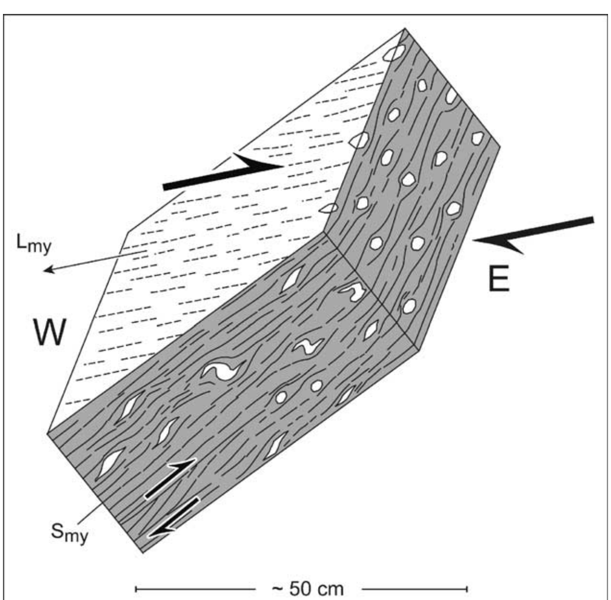

Fig. 9. Simplified schematic block sketch of structural elements in the mylonite zone east of Gastre. The relative sense of shear is indicated by feldspar σ-, single δ-clasts, and S/C fabrics. For location, see Fig. 1.

On the microscale, the foliation of the mylonite strips is recorded by aligned sericite and extremely elongated quartz lenses, which are partly to entirely replaced by subgrains and dynamically generated recrystallization grains. In the mylonitized Gastre suite granite, elongated quartz records relics of former coarse recrystallization grains formed during the initial foliation development (emplacement-related and/or during cooling). Porphyroclasts of K-feldspar and plagioclase in the mylonites exhibit brittle deformation and record alterations to sericite. The relative sense of shear is indicated by displaced feldspar, single S/C fabrics, and shear bands, as well as asymmetric σ-shapes of quartz lenses and pressure shadows at feldspar porphyroclasts (Fig. 7g and h), which confirms the shear sense found in the field. According to the microfabrics, the local mylonite formation took place under lower greenschist metamorphic conditions, whereas single cross-cutting shear planes were formed under brittle conditions.

In the Lipetrén Formation of Sierra de Calcatapul, the NW–SE-trending cataclastic fault line just northeast of Gastre (Fig. 1), indicated as an inferred fault on Proserpio's (1978a) geological map, can be confirmed. It and three additional zones have been interpreted as the main fracture zones of the Gastre fault zone by Rapela et al. (1992). Northeast of Estancia Jaramillo, the fracture zone covers an area farther northeast in the Lipetrén Formation rocks. In different outcrops, however, the various brittle structures do not reveal a clear dextral sense of shear. We could detect no clear offsets of different lithological units in the field, nor are they depicted on the maps.

Furthermore, the few and thin mylonites with different orientations record a variable but not consistent (dextral) sense of shear. Their relations to the cataclastic rocks of the fracture zones are unclear. In general, they do not represent important mylonites that can be related to a large-scale, NW–SE-trending shear zone; the deformed Calcatapul Formation also does not represent a dextral mylonite zone.

6. Age of the Yancamil granite

To provide evidence about the age of the Yancamil granite, a sample for radiometric dating was taken from the Yancamil section ∼20 m southwest of the intrusive contact. There, the coarse-grained granite is slightly deformed and not penetratively foliated. We provide a description of the sample preparation and analytical procedures in Appendix A.

The Yancamil granite is dominated by colorless, clear zircons. Opaque inclusions are scarce, whereas colorless,

Table 1
Isotopic data of zircons from the Yancamil granite

Sample name	Yancamil granite					
Number of grains	3	2	1	3	3	1
U (ppm)	3617.1	2641.9	1299.3	3495.0	4225.8	1194.2
Pb (ppm)	201.7	124.2	57.7	159.7	190.2	55.5
206/204	487.2	303.2	256.9	443.5	314.6	159.3
207/206	0.065109	0.051207	0.051698	0.051681	0.051531	0.051189
Err	0.000204	0.000349	0.000437	0.000446	0.000462	0.000544
207/235 ratio	0.479636	0.313367	0.305511	0.315165	0.299292	0.293702
Err	0.002327	0.002553	0.003013	0.003237	0.003335	0.003979
206/238 ratio	0.053428	0.044383	0.042860	0.044229	0.042124	0.041613
Err	0.000188	0.000168	0.000167	0.000208	0.000247	0.000295
206/238 age (m.y.)	335.5	279.9	270.5	279.0	266.0	262.8
207/235 age (m.y.)	397.8	276.8	270.7	278.2	265.8	261.5
207/206 age (m.y.)	777.9	250.2	272.1	271.3	264.7	249.4
Rho	0.759	0.551	0.531	0.546	0.596	0.627

Notes. Errors are quoted at 1-sigma level.

crystal-shaped (apatite?) needles are frequent, in addition to irregular, bubble-shaped, gas-filled inclusions. The crystal surfaces often show a mother-of-pearl-like luster, which may be due to corrosive attacks after crystallization. Most of the crystals have a short prismatic habit and fractures, and many are broken into pieces. Taking into account the slight deformation of the granite, we believe the fractures are of primary origin and not artifacts of the sample preparation.

The Pupin (e.g. 1988) characteristics of the crystals are dominated by S13/S14 and S8/S9 types. This equilibrium of the forms and the rather high uranium contents of the zircons (ca. 1200 ppm, see Table 1) support the assumption of a hybrid to crustal origin (Pupin, 1992, 1994) for the granite, which is compatible with a Paleozoic arc/backarc situation for the investigated area.

The $^{206}Pb/^{238}U$ and $^{207}Pb/^{235}U$ apparent ages of five of the analyzed zircon fractions (1–3 grains) scatter between 262.8 and 279.9 Ma. Another fraction (3 grains) yields a highly discordant age (Fig. 10a), which we believe is caused by inherited zircons from the intruded country rocks, incorporated into the melt during the injection of the granite.

Assuming recent Pb-loss, the calculated discordia of the five analyses, when forced through a lower intercept of 0, yields an upper intercept age of $261+16/-17$ Ma (MSWD 0.33; Fig. 10b). This Permian age is the probable minimum age of the Yancamil granite.

7. Evolutionary scenario

The structural evidence from the study areas suggests successive stages of events. As the ages, these contrast with previous interpretations and conclusions and can be summarized as follows:

1. Deposition of the Calcatapul Formation. A thick pile of pyroclastic rocks containing reworked clastic and volcanic rocks, along with layers of rhyolite, minor clastic, and metavolcanic rocks (lava flows), makes it possible to infer a depositional area of a magmatic arc or backarc basin. The age of the succession is unclear. On the basis of the geological situation and regional comparisons, a ?Silurian–?Devonian age seems most probable, in accordance with Proserpio's (1978b) interpretation.
2. Granite intrusion. The Calcatapul Formation was intruded by the Yancamil granite. On the basis of the U–Pb dating of zircons from the granite and the relative and absolute ages of the younger igneous rocks, a Late Paleozoic, probably Permian, age for this granite is reasonable.
3. The D_1 deformation of the Calcatapul Formation and Yancamil granite was the result of ~NE–SW compression. In neither unit do we find indications of dextral shearing during this event. Shear sense indicators suggest a relative uplift of the northeastern block parallel to the L_1 lineation. Because the S_1 foliation and slight greenschist facies metamorphism also affected the Permian Yancamil granite but predated the intrusion of the Triassic Lipetrén Formation, a Permian (–?Triassic) age for the D_1 event seems reasonable.
4. The intrusions of the Lipetrén Formation affected the deformed Calcatapul Formation, heterogeneously foliated Yancamil granite, and Gastre suite intrusions. According to the overlying volcanic rocks of the Taquetrén Formation, which presumably spans the Triassic-Jurassic interval, and the ductile D_1 deformation in the study area with the above age, the Lipetrén Formation rocks should be Triassic in age.
5. The local and thin mylonite strips in the Lipetrén Formation do not follow a large-scale, dextral shear zone. The different mylonites may have formed during the same broad interval of compressive deformation, which created the conjugate set of dextral and sinistral C_2 shear planes within the Calcatapul Formation, Yancamil granite, and younger dykes of the Lipetrén Formation.

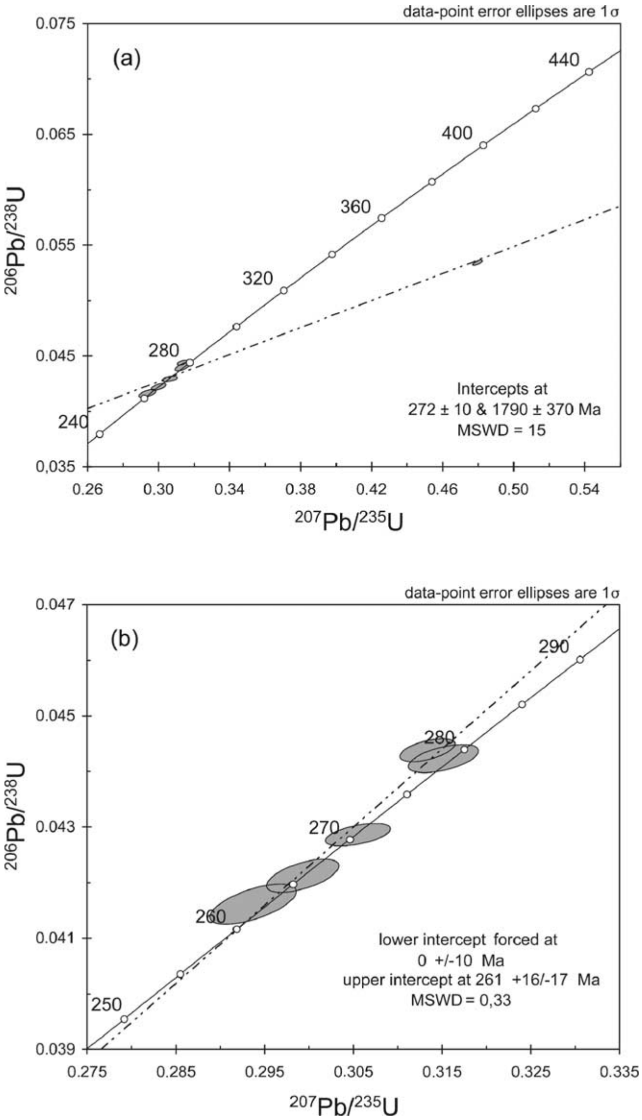

Fig. 10. U–Pb concordia diagrams of zircons of the Yancamil granite. (a) Five nearly concordant analyses from granite zircons and one highly discordant analysis of supposed country rock zircons. (b) 261 + 16/−17 Ma age (95% confidence level) is based on five analyses assuming a recent Pb-loss.

Dextral shear planes dominate in some small parts of the outcrops. In general, a Triassic or younger age for this post-Lipetrén deformation and brittle fracturing along the NW–SE-striking cataclastic zones can be estimated, though additional younger events cannot be excluded.

8. Regional implications and conclusions

In view of its composition, the Calcatapul Formation seems to represent a small cutout of a former magmatic arc or backarc basin environment and thereby indicates ?Early Paleozoic volcanic activity in this western part of north Patagonia. The Permian age of the Yancamil granite must be considered in conjunction with the Late Paleozoic ages of other granitoids in the western part of the North Patagonian Massif, as reported by, for example, Linares et al. (1997), Varela et al. (1999), and López de Luchi et al. (2000). We can only assume that this plutonism was the result of subduction beneath the western Patagonia margin.

In this study, we found no clear indications for the existence of an intracontinental dextral Gastre fault system. This finding applies to the thin mylonite occurrences, which do not depict an overall NW–SE-striking shear zone and are not of regional importance. The Calcatapul Formation indicates a polyphase evolution that comprises several events from the ?Silurian–?Devonian (deposition) to Triassic and/or later times (latest stage deformation). It does not represent a dextral mylonite zone that might be related to a shear zone with regional and plate tectonic significance.

In the NW–SE-striking fracture zones, which depict the wide Gastre fault system, no clear proof of a dextral sense of shear has been reported. As the thin mylonites, they do not record a clear offset of different lithological units. It should be mentioned that various authors have shown sinistral displacements along the main faults of the fault system (e.g. Coira et al., 1975; Nullo, 1978b; Proserpio, 1978b; Volkheimer and Lage, 1981). Detailed field studies from the different faults, however, are still lacking. Furthermore, Proserpio (1978b) and Llambías et al. (1984) describe sinistral faults in the interior of the Sierra del Medio. Llambías et al. (1984) relate the injection of microdioritic dykes with a K–Ar age of 215 ± 10 Ma to this fault tectonics in the sierra.

The overall picture of initial fault tectonics and magmatism has been related to the Triassic episode of rifting (Rapela et al., 1992 and Rapela and Pankhurst, 1992), which produced NW–SE-trending troughs (e.g. Uliana et al., 1989). In contrast, Coira et al. (1975) assume that the onset of sinistral displacements took place during the Late Paleozoic. In the Gastre area, fracturing and local mylonite formation in the Triassic Lipetrén Formation is the only argument for the onset of faulting.

In general, fault tectonics took place and/or continued through post-Late Jurassic, Cretaceous, and Tertiary times (e.g. Volkheimer, 1965, 1973; Coira et al., 1975; Nullo, 1978b, 1979; Rapela and Pankhurst, 1992; Rapela, 1997). In this context, a (subsequent) formation of horst-and-graben structures seems probable, as noted by Volkheimer (1965, 1973) and Llambías et al. (1984) for the latest stage deformation in the Sierra del Medio area. Therefore, we can also interpret the fracture zones of the Gastre fault system as the result of (several stages of) downfaulting of different blocks that led to the formation of distinct young basins.

The evidence from the Gastre area shows no clear indication of the existence of the dextral Gastre fault system as a large-scale structural element. It seems more probable that the fracture zones are related to the formation of depressions (e.g. Pampa de Gastre southwest of Sierra de Calcatapul), which may represent downfaulted basins also outside the study area. Evidence of fracturing and thin mylonite strips is not sufficient for an important dextral lineament. Contrasting interpretations of a sinistral sense of shear or displacements along fracture/fault zones in this part of the North Patagonian Massif do not give a consistent picture and do not support a large-scale, intracontinental, dextral fault system traversing extra-Andean Patagonia.

Acknowledgements

We are grateful to C. Prozzi (Bahía Blanca) for his help and support during fieldwork in Argentina. Discussions with E. Llambías, A. Sato, and P. González (La Plata) improved our understanding of the North Patagonian Massif. Many thanks also to D. Gregori (Bahía Blanca) and J. Ranalli (Mendoza) for all their help and many discussions during fieldwork in Patagonia and to E. Bouhier (Dirección de Minas, San Antonio Oeste/Río Negro) for his support. We thank K. Mezger and his crew (especially H. Beier and E. Trapp) for the opportunity to carry out the isotope work at the Central Laboratory for Geochronology/Institute for Mineralogy of the University of Münster. Many thanks to H. Miller and both reviewers, J.H. Kruhl and R.J. Pankhurst, for their constructive comments and suggestions that helped improve the manuscript. The studies were enabled by grants from the German Research Foundation (DFG, Proj. GO 405/4-1 and 4-2), which are gratefully acknowledged. This article is a contribution to IGCP 436.

Appendix A

A.1. Sample preparation

The cleaned samples were crushed in a jaw breaker to a <10 mm grain size. Further grinding to a grain size of <1 mm was done by a disk mill. The heavy minerals in the sieved fractions of <0.25 mm were concentrated using a Wilfley-type wet shaking table. Further concentration of the zircons was achieved by the use of heavy liquids and a Frantz isodynamic separator. The high-quality zircons for single grain analyses were selected from the bulk sample. No air abrasion was carried out.

A.2. Analytical procedure

The handpicked crystals were washed with 3.5 N HNO_3 for 30 min at 80 °C, then rinsed with distilled water and dried with acetone. Individual crystals and fractions were decomposed with 2 μl 24 N HF in steel-cased multi- or single-hole Teflon containers for 3–4 days at 180 °C. The decomposed zircon was spiked with an appropriate amount (2 μl) of a ^{205}Pb–^{233}U tracer solution. After drying, the sample was converted to the chloride form with 2 μl of 6 N HCl overnight. The dried sample was loaded with a mixture of silica gel, HCl, and phosphoric acid on a Re single filament. Measurement of U and Pb was performed on a VG 354 mass spectrometer equipped with a Daly multiplier and an ion-counting device by peak hopping, with Pb at 1250–1350 °C and U at 1400–1450 °C. Mass fractionation was controlled by the measurement of the standards NBS 982 (0.3%) and U 500 (no mf). The maximum measured ^{206}Pb/^{204}Pb ratio during the course of the analyses was 487 for the fraction (3 grains) with the highest apparent ages, whereas single zircons were at 159.3 and 256.9. This is indicative for a constant and low procedure blank. Calculations were corrected with a maximum Pb blank of 0.01 pg with the following composition: 6/4 = 17.72, 7/4 = 15.52, 8/4 = 37.7 and a U blank of 0.5 pg. The initial Pb composition was calculated according to Stacey and Kramers's (1975) Pb evolution model. The errors in Table 1 and Fig. 10 are quoted at the 1-sigma level, whereas the error of the calculated discordia is given for a 95% confidence level (see Ludwig, 1993).

References

Alonso, G.B., 1987. Resultados geoquímicos y geocronológicos preliminares de los cuerpos graníticos de Pilcaniyeu, Provincia de Río Negro. X Congreso Geológico Argentino (San Miguel de Tucumán), Actas 4, 27–29.

Coira, B.L., Nullo, F., Proserpio, C., Ramos, V.A., 1975. Tectonica de basamento de la region occidental del Macizo Nordpatagónico (Prov. de Río Negro y Chubut) República Argentina. Revista de la Asociación Geológica Argentina 30 (3), 361–383.

Cucchi, R.J., 1993. La Formación Lipetrén en el marco del Gondwana: sector occidental del Macizo Nordpatagónico. XII Congreso Geológico Argentino y II Congreso de Exploración de Hidrocarburos (Mendoza), Actas IV, 105–122.

Dalla Salda, L., Cingolani, C.A., Varela, R., 1990. El basamento de la region occidental del Macizo Norpatagónico, Argentina. XI Congreso Geológico Argentino (San Juan), Actas II, 11–14.

Dalla Salda, L.H., Cingolani, C., Varela, R., 1992a. Early Paleozoic orogenic belt of the Andes in southwestern South America: Result of Laurentia-Gondwana collision?. Geology 20, 617–620.

Dalla Salda, L.H., Dalziel, I.W.D., Cingolani, C.A., Varela, R., 1992b. Did Taconic Appalachians continue into southern South America?. Geology 20, 1059–1062.

Dalla Salda, L., Cingolani, C., Varela, R., 1993. A pre-Carboniferous tectonic model in the evolution of southern South America. Comptes Rendus 12th International Congress on Carboniferous-Permian (Buenos Aires) 1, 371–384.

Dalla Salda, L.H., Varela, R., Cingolani, C., Aragón, E., 1994. The Rio Chico Paleozoic crystalline complex and the evolution of northern Patagonia. Journal of South American Earth Sciences 7 (3/4), 377–386.

Duhart, P., Haller, M., Hervé, F., 2002. Diamictitas como parte del protolito de las metamorfitas de la Formación Cushamen en Río Chico, Provincias de Río Negro y Chubut, Argentina, in: Cingolani, C.A., Cabaleri, N., Linares, E., López de Luchi, M.G., Ostera, H.A., Panarello, H.O. (Eds.), XV Congreso Geológico Argentino (El Calafate/Santa Cruz), Actas II, pp. 97–100.

Franzese, J., Martino, R., 1998. Aspectos cinemáticos y tectónicos de la zona de cizalla de Gastre en la Sierra de Calcatapul, Provincia de Chubut; Argentina. X Congreso Latinoamericano de Geología y VI Congreso Nacional de Geología Económica (Buenos Aires), Actas II, 3.

Franzese, J.R., Pankhurst, R.J., Rapela, C.W., Spalletti, L.A., Fanning, M., Muravchick, M., 2002. Nuevas evidencias geocronológicas sobre el magmatismo gondwánico en el noroeste del Macizo Norpatagónico, in: Cingolani, C.A., Cabaleri, N., Linares, E., López de Luchi, M.G., Ostera, H.A., Panarello, H.O. (Eds.), XV Congreso Geológico Argentino (El Calafate/Santa Cruz), Actas I, pp. 144–148.

Gradstein, F.M., Ogg, J., 1996. A Phanerozoic time scale. Episodes 19 (1, 2), 3–5.

Hoeppener, R., 1955. Tektonik im Schiefergebirge. Geologische Rundschau 44, 26–58.

Linares, E., Cagnoni, M.C., Do Campo, M., Ostera, H.A., 1988. Geochronology of metamorphic and eruptive rocks of southeastern Neuquén and northwestern Río Negro Provinces, Argentine Republic. Journal of South American Earth Sciences 1 (1), 53–61.

Linares, E., Haller, M.J., Ostera, H.A., Cagnoni, M.C., Galante, G., 1997. Radiometric ages of the crystalline basement of the Río Chico region, Ñorquinco department, Río Negro Province, Argentina. South American Symposium on Isotope Geology (Sao Paulo/Brazil, June 15–19, 1997), Extended Abstracts) 1997, 170–175.

Llambías, E.J., Llano, J.A., Rossa, N., Castro, C.E., Puigdomenech, H.H., 1984. Petrografía de la Formación Mamil Choique en la Sierra del Medio-Departamento Cushamen–Provincia del Chubut. IX Congreso Geológico Argentino (San Carlos de Bariloche/Río Negro), Actas 2, 554–567.

López de Luchi, M.G., 1994. Geología de las unidades plutónicas del Macizo Norpatagónico en la zona de Río Chico-Mamil Choique, Provincia de Río Negro, República Argentina. 7 Congreso Geológico Chileno (Concepción), Actas 1, 91–95.

López de Luchi, M.G., Ostera, H., Cerredo, M.E., Cagnoni, M.C., Linares, E., 2000. Permian magmatism in Sierra de Mamil Choique, North Patagonian Massif, Argentina. IX Congreso Geológico Chileno, Actas 2 (4), 750–754.

Ludwig, K.R., 1993. ISOPLOT-Ver.2.70: A plotting and regression program for radiogenic isotope data. US Geological Survey, Open-File Report, 91-445, 42 pp.

Marshall, J.E.A., 1994. The Falkland Islands: a key element in Gondwana paleogeography. Tectonics 13 (2), 499–514.

Nullo, F.E., 1978a. Carta Geológico-Económica de la República Argentina, Hoja 41d, Lipetrén, Provincia de Río Negro (1:200000), Servicio Geológico Nacional, Departamento Carta Geológica, Buenos Aires 1978.

Nullo, F.E., 1978b. Descripción Geológica de la Hoja 41d, Lipetrén, Provincia de Río Negro. Ministerio de Economía, Secretaría de Estado de Minería, Boletín 158, 1–88.

Nullo, F.E., 1979. Descripción Geológica de la Hoja 39c, Paso Flores, Provincia de Río Negro. Ministerio de Economía, Secretaría de Estado de Minería, Boletín 167, 1–79.

Nullo, F., Proserpio, C., 1975. La Formación Taquetrén en Cañadon del Zaino (Chubut) y sus relaciones estratigráficas en el ambito de la Patagonia, de acuerdo a la flora, República Argentina. Revista de la Asociación Geológica Argentina 30 (2), 133–150.

Ostera, H.A., Linares, E., Haller, M.J., Cagnoni, M.C., López de Luchi, M., 2001. A widespread Devonian metamorphic episode in northern Patagonia, Argentina III South American Symposium on Isotope Geology (Sociedad Geológica de Chile, Santiago), Extended Abstracts Volume (CD), pp. 600–603.

Proserpio, C.A., 1978a. Carta Geológico-Económica de la República Argentina, Hoja 42d, Gastre, Provincia del Chubut (1:200000), Servicio Geológico Nacional, Departamento Carta Geológica (Buenos Aires) 1978.

Proserpio, C.A., 1978b. Descripción Geológica de la Hoja 42d, Gastre, Provincia del Chubut. Ministerio de Economía, Secretaría de Estado de Minería, Boletín 159, 1–75.

Pupin, J.P., 1988. Granites as indicators in paleogeodynamics. Rendiconti della Societa Italiana di Mineralogia e Petrologia 43 (2), 237–262.

Pupin, J.P., 1992. Les zircons des granites océaniques et continentaux. Couplage typologie-géochimie des éléments en traces. Bulletin de la Societé Géologique de France 163 (4), 495–507.

Pupin, J.P., 1994. Caracterisation des protolithes des migmatites et granites anatectiques crusteaux d'après l'étude des zircons. Comptes Rendus de l'Academie de Scienes Paris 319 (Serie II), 1191–1197.

Ramos, V.A., 1984. Patagonia: ¿Un continente Paleozoico a la deriva?. IX Congreso Geológico Argentino (San Carlos de Bariloche/Río Negro), Actas II, 311–325.

Ramos, V.A., 1986. Tectonostratigraphy, as applied to analysis of South African Phanerozoic basins by H. De La R. Winter, Discussion. Transactions Geological Society South Africa 89, 427–429.

Rapela, C.W., 1997. El sistema de fallas de Gastre: *e pur si muove*. Revista de la Asociación Geológica Argentina 52 (2), 219–222.

Rapela, C.W., Kay, S.M., 1988. Late Paleozoic to recent magmatic evolution of northern Patagonia. Episodes 11 (3), 175–182.

Rapela, C.W., Pankhurst, R.J., 1992. The granites of northern Patagonia and the Gastre Fault System in relation to the break-up of Gondwana, in: Storey, B.C., Alabaster, T., Pankhurst, R.J. (Eds.), Magmatism and the Causes of Continental Break-Up, Geological Society of London Special Publication, vol. 68, pp. 209–220.

Rapela, C.W., Dias, G.F., Franzese, J.R., Alonso, G., Benvenuto, A.R., 1991. El batolito de la Patagonia central: evidencias de un magmatismo triasico-jurasico asociado a fallas transcurrentes. Revista Geológica de Chile 18 (2), 121–138.

Rapela, C.W., Pankhurst, R., Harrison, S.M., 1992. Triassic 'Gondwana' granites of the Gastre district, North Patagonian Massif. Transactions of the Royal Society of Edinburgh, Earth Sciences 83, 291–304.

Ravazzoli, I.A., Sesana, F.L., 1977. Descripción Geológica de la Hoja 41c, Río Chico, Provincia de Río Negro. Ministerio de Economía, Secretaría de Estado de Minería, Boletín 1977, 1–148.

Richards, P.C., Gatliff, R.W., Quinn, M.F., Williamson, J.P., Fannin, N.G.T., 1996. The geological evolution of the Falkland Islands continental shelf, in: Storey, B.C., King, E.C., Livermore, R.A. (Eds.), Weddell Sea Tectonics and Gondwana Break-up, Geological Society of London Special Publication, vol. 108, pp. 105–128.

Stacey, J.S., Kramers, J.D., 1975. Approximation of terrestrial lead evolution by a two-stage model. Earth and Planetary Science Letters 26, 207–221.

Uliana, M.A., Biddle, K.T., Cerdan, J., 1989. Mesozoic extension and the formation of Argentine sedimentary basins, in: Tankhard, A.J., Balkwill, H.R. (Eds.), Extensional Tectonics and Stratigraphy of the North Atlantic Margins, American Association of Petroleum Geologists, Memoir, vol. 46, pp. 599–614.

Varela, R., Basei, M.A.S., Brito Neves, B.B., Sato, A.M., Teixeira, W., Cingolani, C., Siga, O., 1999. Isotopic study of igneous and metamorphic rocks of Comallo-Paso Flores, Río Negro, Argentina. Actas II South American Symposium on Isotope Geology (Villa Carlos Paz/Córdoba) 1999, 148–151.

Volkheimer, W., 1964. Estratigrafía de la zona extrandina del Departamento de Cushamen (Chubut) entre los paralelos 42° y 42° 30' y los meridianos 70° y 71°. Revista de la Asociación Geológica Argentina 19 (2), 85–107.

Volkheimer, W., 1965. Bosquejo geológico del noroeste del Chubut extraandino (zona Gastre-Gualjaina). Revista de la Asociación Geológica Argentina 20 (3), 326–350.

Volkheimer, W., 1973. Observaciones geológicas en el área de Ingeniero Jacobacci y adyacencias (Provincia de Río Negro). Revista de la Asociación Geológica Argentina 28 (1), 13–36.

Volkheimer, W., Lage, J., 1981. Descripción Geológica de la Hoja 42c, Cerro Mirador, Provincia del Chubut. Ministerio de Economía, Secretaría de Estado de Minería, Boletín 181, 1–71.

Watkeys, M.K., Sokoutis, D., 1998. Transtension in southeastern Africa associated with the Gondwana break-up, in: Holdsworth, R.E., Strachan, R.A., Dewey, J.F. (Eds.), Continental Transpressional and Transtensional Tectonics, Geological Society of London Special Publication, vol. 135, pp. 203–214.